THE ASTROPHYSICAL JOURNAL, 621:1121–1128, 2005 March 10

DETECTION AND DIAGNOSTICS OF A CORONAL SHOCK WAVE DRIVEN BY A PARTIAL-HALO CORONAL MASS EJECTION ON 2000 JUNE 28

A. CIARAVELLA,[1,2] J. C. RAYMOND,[2] AND S. W. KAHLER
AFRL/VSBXS, 29 Randolph Road, Hanscom AFB, MA 01731

A. VOURLIDAS
Naval Research Laboratory, Washington, DC 20375

AND

J. LI
Institute for Astronomy, University of Hawaii, 2680 Woodlawn Drive, Honolulu, HI 96822

Received 2003 December 6; accepted 2004 November 19

ABSTRACT

A fast partial-halo coronal mass ejection (CME) was observed on 2000 June 28 by instruments on the *SOHO* spacecraft. The CME leading edge and filamentary cold core were detected over the northwest limb at 2.32 $R_\odot$ by the *SOHO* UV Coronagraph Spectrometer (UVCS). The broad profile of the O VI λ1032 line gives evidence of a shock front at the leading edge, supporting the identification of white-light CME sharp leading edges as fast-mode shocks. Line-of-sight speeds are as high as 1500 km s^{-1}, comparable to the projected speed obtained from LASCO. Pumping of the O VI λ1032 by Lyβ (v = 1810 km s^{-1}) and of O VI λ1037 by O VI λ1032 (v = 1648 km s^{-1}) were detected, which provide diagnostics of outflow speed and density. The angle of the ejecta with the plane of the sky is obtained, combining the projected speed from LASCO with the line-of sight-speed, and varies between 7° and 46°. In the latter case the projected height of 2.32 $R_\odot$ was at an actual heliocentric distance of 3.6 $R_\odot$. An associated solar energetic particle (SEP) event was observed at the L1 point following this CME. The abundance and charge-state data are consistent with a gradual shock-accelerated SEP event. A type II radio burst was observed at the same time the shock front was detected by UVCS.

Subject headings: Sun: corona — Sun: coronal mass ejections (CMEs) — Sun: UV radiation

1. INTRODUCTION

The "faint circular arc moving out well ahead of the transient loops" observed in the High Altitude Observatory *Solar Maximum Mission* coronagraph observation of 1980 June 29 was interpreted by Gary et al. (1982) as the "manifestation of a shock wave." Later, another white-light observation of a coronal mass ejection (CME)-driven coronal shock was reported by Sime & Hundhausen (1987) in the observations of a CME on 1980 July 6. The authors pointed out that the sides of the CME loop moved laterally and did not form stationary bright columns, or "legs," in the late stage and that raylike features initially outside the CME loop were not deflected until the laterally moving loop sides passed over them. Previous indications of CME-related shocks were reported by Dryer et al. (1979). Their MHD simulation of 1973 August 21 showed an association of the simulated shock with the "forerunner" white-light brightnesses detected by Jackson & Hildner (1978) in *Skylab* coronagraph images. Distant streamer deflections during CMEs, but not interacting directly with the CME fronts, were also the basis on which Sheeley et al. (2000) inferred the existence and propagation of CME-driven shocks. However, the high dynamic range of the Large Angle and Spectrometric Coronagraph Experiment (LASCO; Brueckner et al. 1995) on the *Solar and Heliospheric Observatory* (*SOHO*) might allow the direct observation of CME-driven shock fronts. The problem is to determine when a broad, sharp CME leading edge is a shock and when it is the erupting coronal loop structure. Vourlidas et al. (2003) attacked this problem by examining and simulating a selected observed LASCO CME with a sharp flank resembling a bow shock. Without direct measurements of either the magnetic field or coronal density, the result is not definitive, but Vourlidas et al. (2003) concluded that the CME flank was likely the signature of a fast-mode MHD shock. They showed four other LASCO CMEs with faint but sharp outer envelopes ahead of bright core structures as candidate white-light shocks.

It is currently believed that large gradual ($E \geq 10$ MeV) solar energetic particle (SEP) events observed at or beyond 1 AU are produced by coronal/interplanetary shocks driven by fast CMEs (Reames 1999). This idea is supported by the observed correlation between CME speeds and the logs of peak SEP intensities, but this correlation shows considerable scatter. Some relatively slow ($V_{CME} < 800$ km s^{-1}) CMEs are associated with SEP events, while some fast ($V_{CME} > 1200$ km s^{-1}) CMEs are not SEP associated (Kahler 2001). This suggests that CME speeds are poor proxies for the shocks themselves. A direct observation of a CME-driven shock and the measurement of its properties and their correlations with SEP events (Reames et al. 1997) could be very useful in establishing the necessary or sufficient conditions for shocks to accelerate ambient solar wind or suprathermal ions to SEPs.

The possibility of directly detecting SEP production at coronal shocks by remotely observing broadened profiles of ion line radiation was discussed by Kahler et al. (1999). Subsequently, Raymond et al. (2000) discussed observations with the Extreme Ultraviolet Imaging Telescope (EIT), LASCO, and Ultraviolet Coronagraph Spectrometer (UVCS) instruments on *SOHO* of a coronal shock and fast CME on 1998 June 11. The

[1] INAF-Osservatorio Astronomico di Palermo, Piazza del Parlamento 1, 90134 Palermo, Italy.
[2] Harvard-Smithsonian Center for Astrophysics, 60 Garden Street, Cambridge, MA 02138.

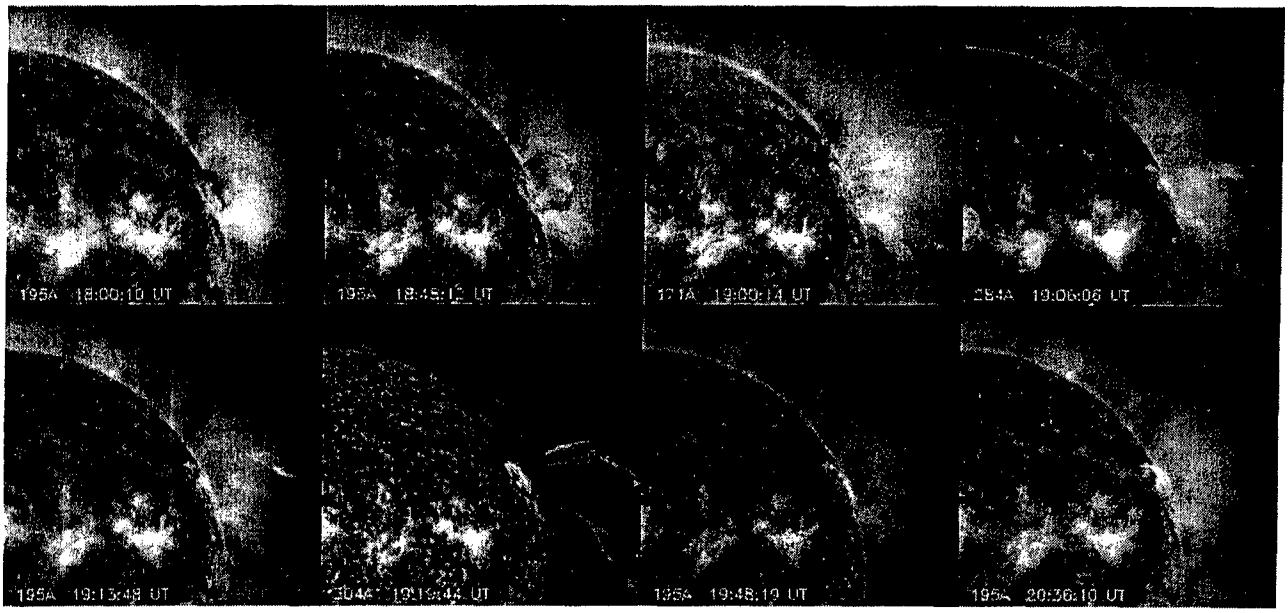

FIG. 1.—CME observed in the EIT wavebands. The 171, 284, and 304 Å images are the only ones available during the eruption. The event was followed in the EIT 195 Å band with a 12 minute cadence except for the times when the other bands were used.

UVCS profiles of O^{5+} and Si^{11+} measured at 1.75 $R_\odot$ were consistent with the modest compression of an MHD shock. Furthermore, a comparison of spectra before and after shock passage showed a line broadening in O^{5+}. Separate but simultaneous type II radio bursts were observed near 30 and 4 MHz, and the shock density deduced from the UVCS observations was consistent with the density of the 30 MHz type II burst. Since that CME was associated with an M1.4 X-ray flare just behind the east limb, it was unfavorably located to produce an SEP event at Earth.

Observations of a fast CME over the west limb on 2000 March 3 were discussed by Mancuso et al. (2002). As with the June 11 shock, a broadening of the O^{5+} line profile measured by the UVCS at 1.7 $R_\odot$ was found after shock passage. The Lyα profile was also broadened, presumably by fast thermalization of hydrogen atoms following resonant charge transfer between fast shocked protons and slow hydrogen atoms. The Lyα profile broadening was consistent with adiabatic compression by the shock, but the O^{5+} broadening was attributed to nonthermal shock effects. The March 3 CME was associated with an M3.8 X-ray flare in AR 8882 at S15° W60°, so it was well located to produce an SEP event at Earth.

We now discuss observations of another CME-driven shock, ahead of a fast west limb CME on 2000 June 28 and accompanied by an SEP event at the Earth. During the event the Sagamore Hill Radio Observatory reported a type II radio burst at the same time (18:58–19:05 UT) as the CME front was crossing the UVCS slit (~18:59–19:06 UT). The original radio data records are no longer available, preventing detailed analysis. However, the reported starting and ending frequencies of 80 and 30 MHz and a model shock speed of 536 km s^{-1} transmitted in an alert message (M. Dryer 2003, private communication) allowed us to deduce preshock density profiles of $n_e = 3 \times 10^6$ to 2×10^7 cm^{-3} and $n_e = (1-8) \times 10^7$ cm^{-3} for the harmonic and fundamental frequency assumptions, respectively. The detection of the shock is confirmed by the UVCS observations, which provide densities, temperatures, and diagnostics of shocks as well.

The 2000 June 28 event was quite bright, as well as fast. Thus, it affords us the opportunity to determine the three-dimensional structure of the CME, along with the pre-CME coronal properties. These are important for measuring the true velocity of the CME and predicting whether and where a shock will form.

The paper is organized as follows. In § 2 we describe the event as observed by different instruments. UVCS spectra of the CME are described in detail in § 3. The three-dimensional structure of the CME is discussed in § 4. The physical parameters of the pre-CME ambient corona are in § 5. Density, temperature, and mass estimates of the CME are described in § 6. The shock front as observed by UVCS is in § 7. The SEP events are in § 8. A discussion and conclusions are in § 9.

2. THE CME ONSET AND PROPAGATION

The June 28 eruption was detected by *SOHO* EIT (Delaboudinière et al. 1995) in the 195 Å band with a cadence of about 12 minutes. One image in each of the other wavelength bands was taken during the event, as shown in Figure 1. The dark arcade oriented along the northwest limb in the first image of Figure 1 started to rise around 18:00:10 UT, and at 18:48:12 UT its projected height was already 0.2 $R_\odot$ above the limb. In the next 195 Å image at 19:13:48 UT the structure had already erupted. The intervening 171 and 284 Å images (Fig. 1, *top row*) already show signs of the eruption. The first sign of CME was detected by UVCS between 18:59:36 and 19:01:36 UT at a position along the slit corresponding to heights 2.34 (polar angle [P.A.] = 287°) to 2.39 $R_\odot$ (P.A. = 281°). The EIT 195 Å 18:48:36 to 19:00:12 UT image ratio shows a bright circular feature extending up to 1.4 $R_\odot$ and surrounding the dark filament. Assuming that this is the front of the CME, we estimate an average speed between EIT and UVCS of 913 km s^{-1} or higher.

Bright strands above the limb in the 171 Å image and knots in the 284 Å image were detected. Similar features can be recognized in the 195 Å image at 19:13:48 UT, and they appear to follow the edges of the thick strands detected in the EIT 304 Å image at 19:19:44 UT. The erupting region was located on the disk very near the west limb and is most probably the prominence

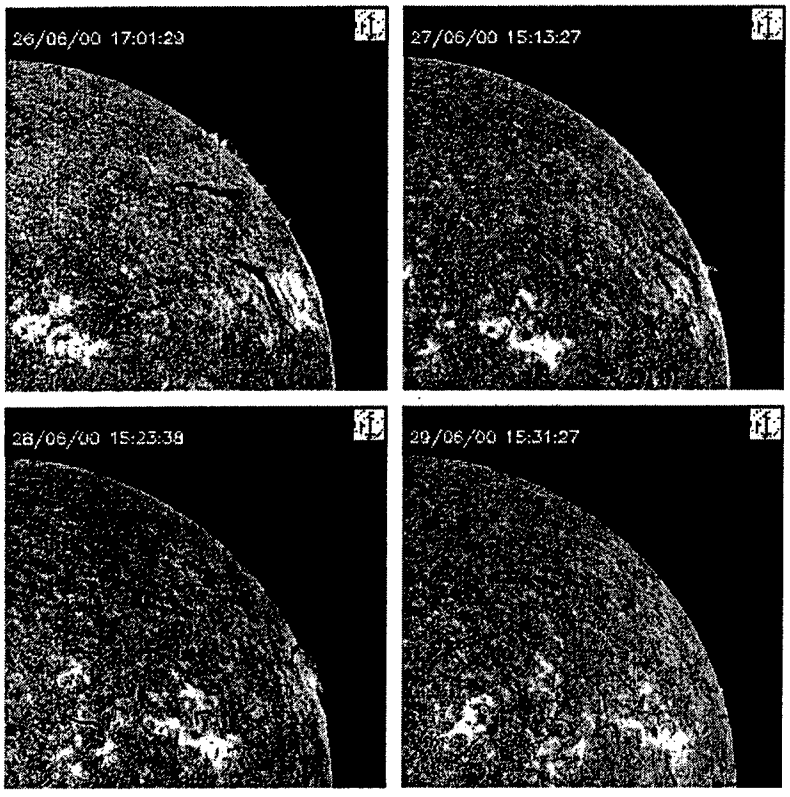

FIG. 2.—BBSO Hα images of the solar northwest quadrant at 1 day intervals. The active region and the two filaments close to the northwest limb are the probable sources of the CME. At the time the CME occurred, the active region and the filament next to it were behind the limb, while the prominence seen at the limb on 2000 June 28 is the most probable source of the eruption.

structure and filament seen in AR 9046 during the preceding days in the Big Bear Solar Observatory (BBSO) Hα images of Figure 2. A C3.7 X-ray flare with an onset at 18:48 and a peak at 19:10 UT was detected by *GOES 8*. After the eruption a large bright arcade formed at the limb at the location where the eruption started (see last two images in Fig. 1). *Yohkoh*/SXT did not observe the eruption, but the SXT image at 19:26:40 UT shows a post-CME arcade with narrow cusps extending above 1.2 $R_\odot$.

The white-light partial halo CME was first seen in the LASCO C2 images at 19:31:55 UT and is shown in Figure 3 as direct and difference images. The difference image shows clearly the faint circular front extending over 180°. At this time the front was already at the edge of the C2 field of view, and its radial extent in the plane of the sky was about 1 $R_\odot$. The direct image shows that the trailing bright region spanned almost 40° and had two components: a diffuse area that seems to be formed by several looplike structures and a lower, more compact bright structure presumed to be filamentary prominence material. The propagation speed of the front between UVCS and the LASCO C2 point at 6 $R_\odot$ was about 1400 km s^{-1}. We determined an average speed of 1433 km s^{-1} and an acceleration of 130 m s^{-2} for the CME front at a P.A. = 270° in the C2 and C3 fields of view. The *SOHO*/LASCO CME catalog gives a lower speed of 1198 km s^{-1} at a P.A. = 294°. The filament inside proceeded more slowly: the strands detected by UVCS moved with an average speed of 800 km s^{-1} and an acceleration of 100 m s^{-2}.

3. THE UVCS OBSERVATIONS

The UVCS (Kohl et al. 1995) entrance slit was centered over the northwest limb at P.A. = 295° and a heliocentric height of 2.32 $R_\odot$ (Fig. 3) from 15:32 UT on June 28 until 12:24 UT on June 29. The exposure time was 2 minutes, and the field of view of the entrance slit was 50 μm (14″) wide and 41′ long. The detector was masked to select three wavelength ranges, 1024–1045, 976–979, and 1210–1220 Å. The spectral binning was 2 pixels, corresponding to 0.198 Å in the first two ranges and 0.183 Å in the third. The main lines in those ranges are the O VI λλ1032, 1037 doublet, the C III λ977, H I Lyα and Lyβ, and O V] λ1218 lines, and in second order the lines of Mg X λ610 and Si XII λ520. Along the entrance slit the detector was binned to 3 pixels, corresponding to 21″. The spectral lines detected in the CME material are the O VI doublet, Lyα, Lyβ, C III, and O V]. No Mg X or Si XII emission was observed during the CME.

The O VI λλ1032, 1037 and the H I Lyα are the only spectral lines that provide a complete view of the event. The fragments of the ejecta with the highest Doppler shifts were not detected in the C III and Lyβ lines because they fell outside the selected wavelength ranges. On the other hand, O V] was observed in a small portion of the ejecta. In Figure 4 we show the images of the CME observed through the UVCS slit in the O VI λ1032 and H I Lyα lines. The vertical axis is the UT time with the start of the observation at the top. The P.A. along the UVCS slit is given on the horizontal axis. Note that Figure 4 would correspond to images of the CME if all the ejecta moved at a constant speed perpendicular to the slit. Overall, the O VI λ1032 and H I Lyα images look similar except for the curved thread around 20:41 UT extending up to P.A. = 300° in the O VI image. This feature is barely detected in Lyα up to 290°. The area around P.A. = 295° is instead very bright in the O V] λ1218 (not shown). The O V] λ1218 to O VI λ1032 ratio near 5.3 indicates an ionization

FIG. 3.—First LASCO C2 observation of the CME in the difference (*top*) and direct (*bottom*) images. In the top panel the EIT 304 Å image at 19:19:44 UT and the position of the UVCS slit are also shown. The difference image shows the front of the CME extending over 180°.

temperature between 2.4 and 3.4×10^5 K. The dark gap seen at the top of the Lyα image at P.A. = 280°–283° corresponds to highly blueshifted plasma that fell outside the selected spectral range and therefore was not detectable.

The temporal evolution of the UV spectra can be summarized as follows. At 18:59:36 UT between P.A. = 281° and 287° the O VI line profiles become very broad and blueshifted, although they remain relatively faint. This broad blueshifted emission corresponds to the CME front. At 19:03:57 more clumpy material appears along the slit, and its Doppler shift increases toward the center of the slit. The spatial and spectral distributions of this component most likely reflect the structure of the bright material just behind the front that in LASCO images appears as a set of overlapping loop structures (see the direct image in Fig. 3). With a difference time of 4 minutes and 23 s between the shock front and the arrival of the bright loops and a speed of 1400 km s^{-1}, we obtain a standoff distance of 0.53 $R_\odot$ between the shock and the other part of the CME. At 19:06:06 UT the denser and colder prominence core starts to enter the UVCS slit from the southern edge and progressively extends through one-half the slit. This plasma is initially blueshifted up ~1500 km s^{-1} in the O VI lines. Later blue- and redshifted components are

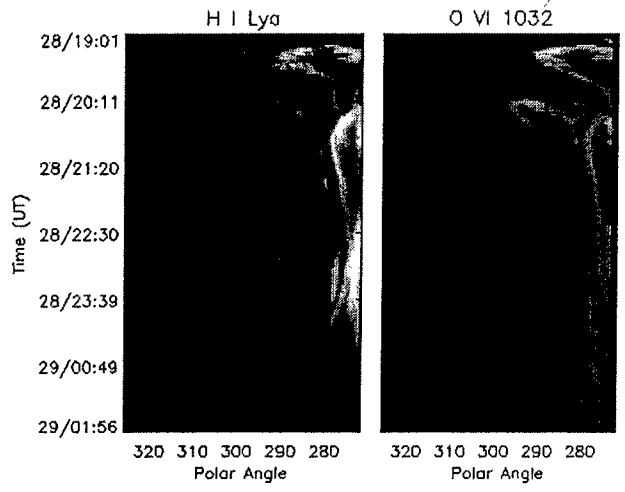

FIG. 4.—UVCS images of the CME in Lyα and O VI 1032 Å lines. The vertical axis is the observation time and the horizontal axis the P.A. along the slit. The times in the images run from 2000 June 28 19:01:48 UT (*top*) to 2000 June 29 01:56:32 UT (*bottom*).

simultaneously detected, and finally the trail of the ejecta shows very small Doppler shift. Such a Doppler shift evolution is frequently observed in UV spectra of CMEs (Ciaravella et al. 1997, 2000).

4. THE THREE-DIMENSIONAL STRUCTURE OF THE CME

The true speed of the CME is a combination of the speed in the plane of the sky and the speed along the line of sight. An important contribution from the UV spectra is the diagnostics of the line-of-sight and outflow speed that allow for a three-dimensional reconstruction of the CME. In particular, the Doppler shifts of the lines provide the line-of-sight speed that can be combined with the plane-of-the-sky component to obtain the true outflow speed of the ejecta. In addition, the radiatively scattered lines provide indicators of the range of outflow speed as well. The Doppler shift image of the CME in the O VI λ1032 line is shown in Figure 5. It is important to mention that the Doppler shift of radiative lines is underestimated by the usual formula $v = c\Delta\lambda/\lambda$ if the emitting plasma is far from the plane of the sky and if radiative scattering dominates over collisional excitation (Noci & Maccari 1999). Thus, the line-of-sight speeds of Figure 5 could be higher.

The CME material detected by UVCS was initially very highly blueshifted, and later in the observation the trail of the ejecta showed very small shifts. Between 20:15:33 and 20:48:01 UT at P.A. = 273° a slightly redshifted (115 km s^{-1}) feature was detected simultaneously with the blueshifted material. In Figure 5 we show the redshifted part only. The high-speed component along the line of sight suggests that the prominence core of the CME is quite far from the plane of the sky. Such high blueshifts were also observed in the front and the diffuse material just behind it (Fig. 3, but not shown in Fig. 5). In those components the blueshift increases from 170 km s^{-1} at P.A. = 278° to 1500 km s^{-1} at P.A. = 296°, implying that the entire structure is tilted toward the observer. With a speed in the plane of the sky of ~1400 km s^{-1}, the angle with the plane of the sky varies between 7° (P.A. = 278°) and 46° (at P.A. = 296°). Thus, the ejecta observed along the slit at a projected height of 2.32 $R_\odot$ (P.A. = 296°) were at an actual heliocentric distance of up to 3.6 $R_\odot$. With an angle of 46° and a distance of

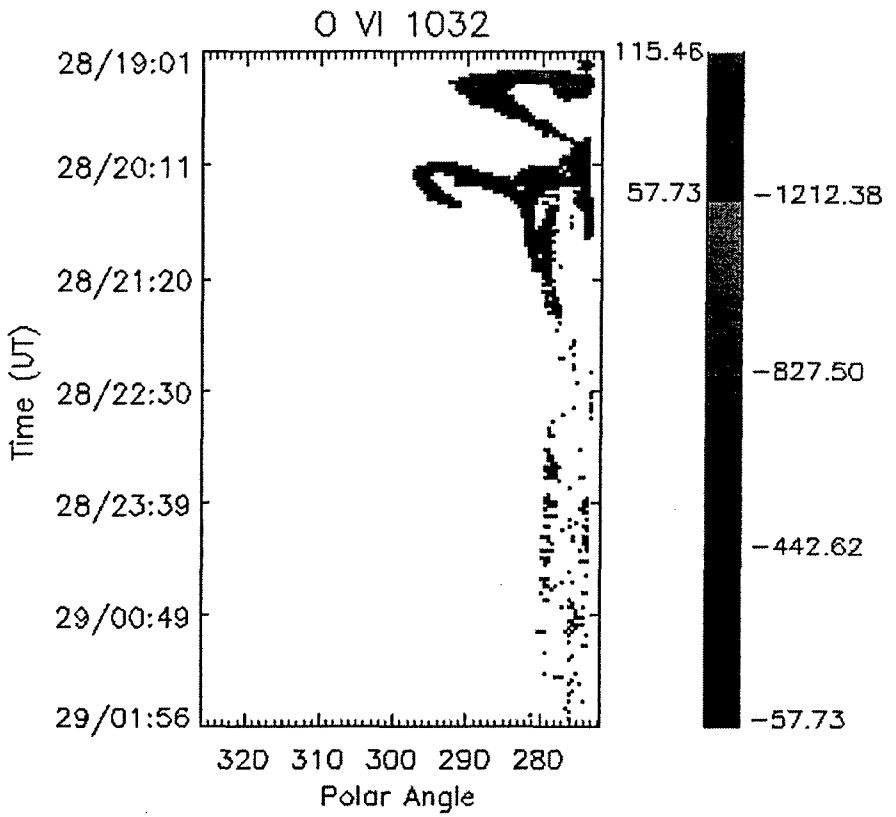

FIG. 5.—Doppler shift image of the CME in the O VI λ1032 line. The blueshift (*blue*) and redshift (*red*) ranges are plotted in the color bar on the right.

3.6 $R_\odot$, the ejecta are 2.6 $R_\odot$ away from the plane of the sky. Thus, the width of the CME core along the line of sight is even larger than the projected width in the plane of the sky (about 1 $R_\odot$).

Starting from 22:30 UT on June 28 along the edges of the trail of the emission, very small blue- and redshifts ($v \leq 115$ km s^{-1}; see Fig. 5) are detected. The consistent difference of about 30 km s^{-1} between the north and the south edges of the trail suggests rotational motion such as an untwisting of a helical structure (e.g., Ciaravella et al. 2000). In the LASCO C2 images taken between 22:06 and 23:06 UT the northern filament thread (P.A. = 224°–226°) shows a morphological signature of possible untwisting structure that is consistent with UVCS Doppler shifts.

As discussed in § 6 there are fragments of the prominence core where pumping of the O VI λ1032 by Lyβ and O VI λ1037 by O VI λ1032 or by C II $\lambda\lambda$1037.02, 1036.94 has been detected (see Fig. 2 of Raymond & Ciaravella 2004). This circumstance implies that the outflow speeds are in the range 1600–1800 km s^{-1}, significantly higher than the average speed in the plane of the sky measured from LASCO images.

5. PRE-CME STREAMER PARAMETERS

This knowledge of the UV spectrum of the pre-CME corona is a unique opportunity to determine the physical conditions, such as density, temperature, and ionization stage, where the shock front propagates and develops. These diagnostics are also important for comparison with the charge states detected in the SEP observations and the densities obtained from type II radio bursts.

In the solar corona the Lyα and O VI $\lambda\lambda$1032, 1037 lines have both collisional and radiative components. The latter arises from resonant scattering of the intense lines formed in the lower atmospheric layers. In addition to the temperature, density, and abundance, their resonantly scattered components are sensitive to the outflow speed of the emitting plasma. A resonantly scattered line is Doppler dimmed as the profile of the absorbing material is shifted with respect to the exciting radiation. The range of sensitivity to the outflow speed depends on the profiles of the absorbing lines, and these are generally different for Lyα and O VI lines. The O VI λ1032/λ1037 ratio is 2:1 for the collisional components and 4:1 for radiative components. The ratio of Lyα to Lyβ is 7.6:1 for the collisional component at high temperature, while that for the radiative component is 570:1 (Raymond et al. 1997, 2002). The relative intensities of these components can be used to determine electron densities and outflow speeds (Withbroe et al. 1982; Noci et al. 1987). In the static corona the radiative pumping is done by the same observed lines, and the line ratio is strictly a density diagnostic.

The O VI doublet ratio in the pre-CME streamer, averaged over 71 exposures and 18′along the slit, is 3.38 ± 0.03. We take the O VI disk intensities to be 1.94×10^{13} photons cm^{-2} s^{-1} sr^{-1} based on the solar minimum surface brightnesses given by Raymond et al. (1997) and a factor of 1.8 enhancement for the near maximum conditions of June 2000 (Rottman et al. 2001). Thus, the doublet ratio implies a density of 2×10^6 cm^{-3}.

Using UVCS spectra and the CHIANTI version 3.02 (Dere et al. 2001) emissivity table we can compute the ionization state of the pre-CME corona. Line intensities of three low first ionization potential elements, Fe X λ1028.04 (6.44×10^6 photons cm^{-2} s^{-1} sr^{-1}), Si XII λ520.66 (4.03×10^7 photons cm^{-2} s^{-1} sr^{-1}), and Mg X λ609.76 (1.47×10^9 photons cm^{-2} s^{-1} sr^{-1}), yield a temperature of 1.3×10^6. At this temperature

$O^{+6}/O^{+5} = 292$ and $O^{+7}/O^{+6} = 0.06$. The Fe x λ1028.04 to O VI λ1032 ratio at 1.3×10^6 shows that the abundance ratio Fe/O is 0.24, a factor of 4 higher than the photospheric value of 0.06 (Allen 1973, p. 31).

6. CME EJECTA IN UV LINES: DENSITY AND MASS ESTIMATES

The high speed of the June 28 CME presents a unique density diagnostic that has been used by Raymond & Ciaravella (2004) to derive plasma densities. For the high-speed portion of the ejecta where this technique applies, the densities range from 3.6×10^6 to 4×10^7 cm^{-3}. In this portion of the ejecta O VI λ1032 reaches intensities of 4×10^{11} photons cm^{-2} s^{-1} sr^{-1}. For densities around 2×10^7 cm^{-3} as derived above, this implies a depth of about 0.1 $R_\odot$ if the emitting gas is near 3×10^5 K (as assumed in the density estimate), and the ionic concentration of O VI is near that in ionization equilibrium. The scale of these features along the slit is also about 0.1 $R_\odot$. However, the fainter emission in different parts of the slit and the coherent motion of groups of bright knots along the slit from one exposure to another suggest that these are parts of an emitting sheet of plasma rather than individual cylindrical threads. It is not clear whether the bright features are denser regions within the sheets or regions where the sheet happens to be nearly tangent to the line of sight.

We can estimate the mass of the brightest portion of the CME observed by UVCS where the density diagnostics mentioned above apply. This part of the ejecta goes from the top of the images in Figure 4 down to 20:54:31 UT. In computing the mass from the density map we need to convert the UVCS time series (vertical axis in Fig. 4) to spatial coordinates by multiplying the speed at each position along the slit by the exposure time. The plane-of-the-sky speed map we used was obtained assuming that the all ejecta left the Sun at the same time (18:48:36 UT) and reached the UVCS slit after traveling a time given by the difference between the UVCS detection time and 18:48:36 UT. In this scenario the speed declines from $\sim$1200 km s^{-1} at the top of the image in Figure 4 to 110 km s^{-1} at 20:54:31 UT. This portion of the image is where we have density diagnostics. A thickness of 0.1 $R_\odot$ along the line of sight was used (see Raymond & Ciaravella 2004). Under these assumptions we estimate a mass of 1.7×10^{12} g. This mass is only about $\frac{1}{3}$ of the mass detected by UVCS because the portion of the ejecta used for this estimate is less than one-third of the ejecta detected between 19:06:06 and 20:54:31 UT.

The total mass of the event obtained from C3 images is $\sim 7 \times 10^{15}$ g, a typical value for a large CME. From C2 images the portion of CME observed by UVCS ranges between 7.3×10^{14} and 8.3×10^{14} g if the ejecta are either in the plane of the sky or 45° from the plane of the sky, respectively.

The mass observed by UVCS is only a small fraction of the values obtained from C2 in the same portion of the CME. Several factors contribute to this low estimated mass. First, the plane-of-the-sky speed used is too low for most of the ejecta. Second, where the O VI ratio is too close to 2 the density diagnostics is not valid. Another important factor is that the O VI lines, used for the density diagnostics, are sensitive to plasma in a certain range of temperature. We assumed that the O VI is formed near its ionization equilibrium peak at 3×10^5 K. However, the plasma may be far from equilibrium (Akmal et al. 2001; Ciaravella et al. 2001). If $T \sim 50{,}000$ K, the collisional excitation rate would be about 10 times smaller and the required density 10 times larger. However, even taking into account these factors, the mass observed by UVCS is still a small fraction of the mass estimated from LASCO. This is most probably the reason why the in situ observations do not easily detect low-ionization material (Lepri & Zurbuchen 2004).

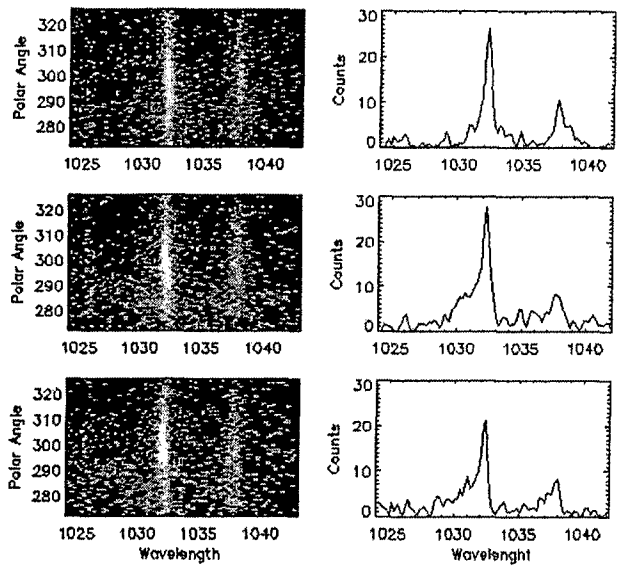

FIG. 6.—UVCS spectra taken between 18:59:36 (*top*) and 19:05:57 UT (*bottom*). The main lines of the spectrum are the O VI $\lambda\lambda$1032, 1037. The vertical coordinate is the polar angle along the entrance slit. The blueshifted emission from the front has a profile much wider than that of the background corona (narrow component). As the front passes through the slit the wide component is detectable along a lager portion of the slit. *Right:* Line profiles in the portion along the slit between P.A. = 281° and 287°.

7. THE SHOCK FRONT

The duration and the time of the broad and blueshifted component (see Fig. 6), detected for three consecutive exposures starting at 18:59:36 UT, are consistent with the passage of the circular faint shock front. This shock was associated in time with the type II burst and the SEP event. The front projected thickness in the C2 image at 19:33:55 UT (see Fig. 3) is almost 1 $R_\odot$, and for a speed of 1400 km s^{-1} or higher it would take at most four exposures to cross the UVCS slit before the edge of the core would be detected. We detected the broad O VI profiles for only three exposures before the brighter clumpy core material reached the UVCS slit. Taking into account that expansion may take place during the time the CME travels between the UVCS slit and the edge of the C2 field of view, the UVCS observations are consistent with this interpretation.

In the same portion of the slit where the front was detected the Lyα line intensity decreases by $\sim$30%. A faint blueshifted emission is also detected that corresponds to the H I Lyα emission from the expanding front. At 19:01:48 UT a broad streak appears in the Si XII λ520 image but with poor statistics. An upper limit to the line intensity is 1.7×10^9 photons cm^{-2} s^{-1} sr^{-1}. The pre-CME value is $\sim 9 \times 10^7$ photons cm^{-2} s^{-1} sr^{-1}.

The O VI $\lambda\lambda$1032, 1037 spectra from 18:59:36 to 19:05:57 UT are in Figure 6 along with the λ1032 line profile in the portion of the slit between P.A. 281° and 287°. The O VI λ1032 broad component of Figure 6 (*middle*) has a $v_{1/e} = 393 \pm 49$ km s^{-1} and the narrow background corona component has $v_{1/e} = 100 \pm 5$ km s^{-1}. While the narrow component traces the almost undisturbed streamer material along the line of sight, the broad component is emitted by the plasma inside the CME front that is expanding outward after being heated by the shock passage.

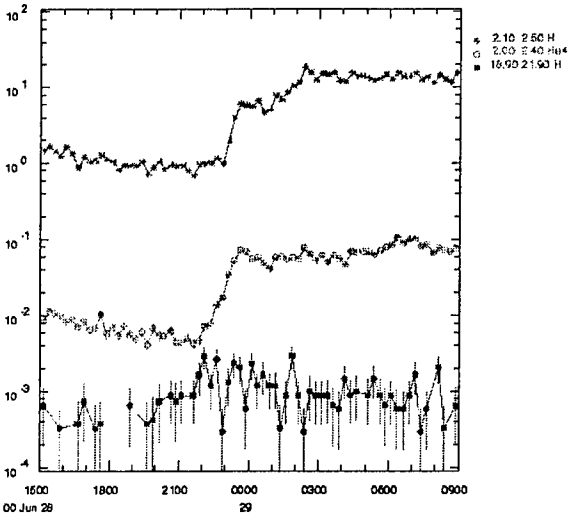

FIG. 7.—Intensities of the June 28–29 SEP event from the EPACT experiment on *Wind*.

The expansion speed could in principle be estimated from the white-light data, but the results depend on the selected portion of the front and are determined at heights much greater than that of the UVCS slit position. As an alternative estimate we consider a spherical front going through the UVCS slit. Each ion contributes to the detected line profile with a speed that depends on its position along the front. The FWHM of the emission line depends on $v \sin(\theta/2)$, where θ is the angle of the front portion intercepted by the slit. The fraction of the front we consider in Figure 6 is $\sim 5°$ wide, and for an outflow speed of 1400 km s^{-1} the expected FWHM of the emission line would be $\sim$244 km s^{-1}. The difference in quadrature between the measured width and the expansion width gives an FWHM of 602 km s^{-1}, which, if considered as a thermal width, implies an oxygen kinetic temperature of 1.2×10^8 K.

8. THE SEP EVENT

A $\sim$20 MeV solar energetic proton event with a peak intensity of 2×10^{-3} photons cm^{-2} s^{-1} sr^{-1} MeV^{-1} and an onset on June 28 between 20:00 and 20:30 UT was observed with the Energetic Particles: Acceleration, Composition, and Transport (EPACT; von Rosenvinge et al. 1995) instrument on *Wind*. The velocity dispersion between the onsets of the $\sim$2 and $\sim$20 MeV protons shown in Figure 7 makes clear that this is a transient SEP event. The observed Fe/O ratio of $\sim$0.1 at $\sim$3 MeV nucleon^{-1} establishes this as a gradual, hence shock-accelerated, SEP event (Reames 1999). Assuming a total proton path length of 1.3 AU based on an observed solar wind speed of $\sim$480 km s^{-1}, we calculate the solar injection time for the 20 MeV protons to be $\sim$19:15–19:45 UT. The measured height of the CME leading edge was less than 8 $R_\odot$ during this time interval. The EPAM instrument aboard *ACE* showed an SEP onset near 19:00 UT, further restricting the height of the CME leading edge to less than 4 $R_\odot$ or very close to the time the shock crossed the UVCS slit.

The O and Fe charge states determined for the SEP event from the Solar Energetic Particle Ionic Charge Analyser (SEPICA; Möbius et al. 1998) on the *ACE* spacecraft were 5.9 and 10.2, respectively (M. Popecki 2003, private communication), in the $E \lesssim 0.5$ MeV nucleon^{-1} range. The Fe charge state was comparable to those of four large gradual SEP events observed in 2000 (Popecki et al. 2003) and consistent with a thermal equilibrium temperature of 1×10^6 K. In the June 29–30 period the solar wind O^{+7}/O^{+6} ratio measured by SWICS ranges from 0.2 to 0.4.

9. DISCUSSION

The coronal shock wave of the 2000 June 28 CME is the third known case in which a CME-driven shock has been observed by the UVCS slit. Table 1 is a comparison of the characteristics of the June 28 event with those of 1998 June 11 (Raymond et al. 2000) and 2000 March 3 (Mancuso et al. 2002). The listed CME speeds are the ones directly measured by the authors, and in parentheses are those speeds given in the *SOHO* LASCO CME Catalog. All three CMEs were fast and broad, statistically likely to be associated with both metric and decameter to hectometer (DH) type II shocks (Lara et al. 2003), although no DH type II burst was associated with either the March 3 or the June 28 CMEs. The UVCS preshock densities were consistent with those of the June 11 and March 3 metric type II bursts. In the case of 2000 June 28 the radio data were lost, and since often their interpretation is controversial, we are unable to make a detailed comparison. However, there is a good association in time with the signatures of shock detected in the UVCS spectra.

The 2000 June 28 shock front was observed at a higher projected and actual heliocentric distance than those of 1998 June 11 and 2000 March 3 (Table 1). Aside from the low statistics in the Si XII line, which is most probably due to the height, similar characteristics are detected in the spectral lines. The decrease in the Lyα intensity and the broad O VI profile indicate

TABLE 1

PROPERTIES OF CMEs WITH OBSERVED SHOCKS

Property	1998 June 11[a]	2000 March 3[b]	2000 June 28
First UVCS shock observation (UT)	10:10	2:19	18:59
Height of UVCS slit center ($R_\odot$)	1.75	1.7	2.32
CME speed[c] (km s^{-1})	1200 (1223)	920 (841)	1433 (1198)
Solar source region	East limb	S15° W60°	Northwest limb
CME angular width[c] (deg)	177	98	134
O VI $v_{1/e}$ line broadening (km s^{-1})	541	400	393
I(20 MeV) (p cm^{-2} s sr MeV)	None	0.008	0.002
Metric type II burst (UT)	10:11–10:19	2:14–2:30	18:58–19:05
DH type II burst (UT)	10:15–10:20	None	None

[a] From Raymond et al. (2000).
[b] From Mancuso et al. (2002).
[c] Widths and (speeds) from the *SOHO* LASCO CME Catalog.

that also in the June 28 event the O ions are preferentially heated by the shock.

Another important contribution from the CME spectra is the diagnostics of the line-of-sight and outflow speed that allow for a three-dimensional reconstruction of the event. The Doppler shift detected in the ejected plasma allowed us to compute the angle between the direction of the CME ejecta and the plane of the sky and therefore the actual heliocentric distance of the ejecta. In the June 28 event we estimated from the Doppler shifts that the portion of front observed at a projected height of 2.32 $R_\odot$ was at an actual heliocentric distance of 3.6 $R_\odot$. This implies an angle with the plane of the sky of $\sim 46°$.

The O VI $\lambda\lambda$1032, 1037 doublet ratio shows that pumping of the O VI λ1032 line by Lyβ and of O VI λ1037 by O VI λ1032 and C II occurs in some fragments of the ejecta. The required outflow speeds range from 170 up to 1800 km s^{-1}. This pumping provides density estimates in the range 1.3×10^6 to 4×10^7 cm^{-3} (Raymond & Ciaravella 2004).

The sharp and smooth white-light fronts of each of the CMEs of Table 1 (Fig. 1 of Raymond et al. 2000, Fig. 1 of Mancuso et al. 2002, and Fig. 3) are similar to that of the 1999 April 2 CME observed in LASCO and simulated by Vourlidas et al. (2003), who concluded that that front and the fronts of four similar CME candidates were fast-mode MHD shocks. For faster CMEs confirmation of the presence of shocks would be associated DH type II bursts (Gopalswamy et al. 2001), which were reported by the *Wind*/WAVES experiment[3] for only one of the three CMEs of Table 1 and none of the five CMEs presented by Vourlidas et al. (2003). However, the UVCS detection of the heating of the O^{+5} ions at the white-light fronts of the three CMEs of Table 1 supports the Vourlidas et al. (2003) conclusion that the sharp white-light fronts are CME-driven MHD shocks.

[3] See http://lep694.gsfc.nasa.gov/waves/waves.html.

While it is known that type II bursts are produced by shocks, it is not known what fraction of shocks produces detectable type II emission.

In § 8 we discussed the SEP event associated with the June 28 shock event. Because of its location on the east limb, no observable SEP event was expected at Earth following the June 11 CME, but an SEP event with a 1 AU onset at ~03:00 UT was associated with the March 3 west limb CME (Table 1), although that event was not included in the Mancuso et al. (2002) work. The UVCS observations of O VI line broadening at shock fronts have important implications for the remote detection of SEP acceleration (Kahler et al. 1999). The MeV SEP speeds ($v \gtrsim 5 \times 10^5$ km s^{-1}) exceed by 3 orders of magnitude the $v \sim 500$ km s^{-1} speeds of the O VI line broadenings of the events of Table 1. Nevertheless, the line broadenings may prove to be proxies of shock acceleration to the higher MeV energies, allowing the remote detection of times and places of SEP acceleration. DH type II bursts are shock signatures well associated with SEP events (Cliver et al. 2004), but many small SEP events, such as the two cases of Table 1, are not associated with the DH type II bursts. Further work could show that observations of shock heating are signatures of SEP events.

This work was supported by NASA grant NAG5-12827 to the Smithsonian Astrophysical Observatory. We acknowledge use of the LASCO CME catalog. This CME catalog is generated and maintained by the Center for Solar Physics and Space Weather, the Catholic University of America in cooperation with the Naval Research Laboratory, and NASA. *SOHO* is a project of international cooperation between ESA and NASA. We thank Master Sergeant S. Straw for his help with the metric radio data from the Sagamore Hill Radio Observatory, D. Reames for the EPACT SEP data, and M. Popecki for his analysis of the SEPICA data.

REFERENCES

Akmal, A., Raymond, J. C., Vourlidas, A., Thompson, B., Ciaravella, A., Ko, Y.-K., Uzzo, M., & Wu, R. 2001, ApJ, 553, 922
Allen, C. W. 1973, Astrophysical Quantities (3rd ed.; London: Athlone)
Brueckner, G. E., et al. 1995, Sol. Phys., 162, 357
Ciaravella, A., Raymond, J. C., Reale, F., Strachan, L., & Peres, G. 2001, ApJ, 557, 351
Ciaravella, A., et al. 1997, ApJ, 491, L59
———. 2000, ApJ, 529, 575
Cliver, E. W., Kahler, S. W., & Reames, D. V. 2004, ApJ, 605, 902
Delaboudinière, J.-P., et al. 1995, Sol. Phys., 162, 291
Derc, K. P., Landi, E., Young, P. R., & Del Zanna, G. 2001, ApJS, 134, 331
Dryer, M., Wu, S. T., Steinolfson, R. S., & Wilson, R. M. 1979, ApJ, 227, 1059
Gary, D. E., Dulk, G. A., House, L. L., Wagner, W. J., Illing, R. I., Sawyer, C., & McLean, D. J. 1982, Adv. Space Res., 2, 253
Gopalswamy, N., Yashiro, S., Kaiser, M. L., Howard, R. A., & Bougeret, J.-L. 2001, J. Geophys. Res., 106, 29219
Jackson, B. V., & Hildner, E. 1978, Sol. Phys., 60, 155
Kahler, S. W. 2001, J. Geophys. Res., 106, 20947
Kahler, S. W., Raymond, J. C., & Laming, J. M. 1999, in AIP Conf. Proc. 471, Solar Wind Nine, ed. S. R. Habal et al. (Woodbury: AIP), 685
Kohl, J. L., et al. 1995, Sol. Phys., 162, 313
Lara, A., Gopalswamy, N., Nunes, S., Muñoz, G., & Yashiro, S. 2003, Geophys. Res. Lett., 30, 8016, DOI: 10.1029/2002GL016481
Lepri, S. T., & Zurbuchen, T. H. 2004, J. Geophys. Res., 109, A01112
Mancuso, S., Raymond, J. C., Kohl, J., Ko, Y.-K., Uzzo, M., & Wu, R. 2002, A&A, 383, 267
Möbius, E., et al. 1998, Space Sci. Rev., 86, 449
Noci, G., Kohl, J. L., & Withbroe, G. L. 1987, ApJ, 315, 706
Noci, G., & Maccari, L. 1999, A&A, 341, 275
Popecki, M. A., Moebius, E., Morris, D., Klecker, B., & Kistler, L. M. 2003, in Proc. 28th Int. Cosmic Ray Conf. (Japan), 6, 3287
Raymond, J. C., & Ciaravella, A. 2004, ApJ, 606, L159
Raymond, J. C., et al. 1997, Sol. Phys., 175, 645
———. 2000, Geophys. Res. Lett., 27, 1439
———. 2002, ApJ, 564, 1054
Reames, D. V. 1999, Space Sci. Rev., 90, 413
Reames, D. V., Kahler, S. W., & Ng, C. K. 1997, ApJ, 491, 414
Rottman, G., Woods, T., Snow, M., & DeToma, G. 2001, Adv. Space Res., 27, 1927
Sheeley, N. R., Jr., Hakala, W. N., & Wang, Y.-M. 2000, J. Geophys. Res., 105, 5081
Sime, D. G., & Hundhausen, A. J. 1987, J. Geophys. Res., 92, 1049
von Rosenvinge, T. T., et al. 1995, Space Sci. Rev., 71, 155
Vourlidas, A., Wu, S. T., Wang, A. H., Subramanian, P., & Howard, R. A. 2003, ApJ, 598, 1392
Withbroe, G. L., Kohl, J. L., Weiser, H., & Munro, R. H. 1982, Space Sci. Rev., 33, 17

REPORT DOCUMENTATION PAGE

Form Approved
OMB No. 0704-0188

1. REPORT DATE *(DD-MM-YYYY)*
17-01-2006

REPRINT

4. TITLE AND SUBTITLE
Detection and Diagnostics of a Coronal Shock Wave Driven by a Partial-Halo Coronal Mass Ejection on 2000 June 28

5a. CONTRACT NUMBER

5b. GRANT NUMBER

5c. PROGRAM ELEMENT NUMBER
61102F

6. AUTHOR(S)
Ciaravella, A.*, J.C. Raymond**, S.W. Kahler, A. Vourlidas#
J. Li##

5d. PROJECT NUMBER
2311

5e. TASK NUMBER
RD

5f. WORK UNIT NUMBER
A1

7. PERFORMING ORGANIZATION NAME(S) AND ADDRESS(ES)
Air Force Research Laboratory/VSBXS
29 Randolph Road
Hanscom AFB MA 01731-3010

8. PERFORMING ORGANIZATION REPORT NUMBER
AFRL-VS-HA-TR-2006-1006

9. SPONSORING / MONITORING AGENCY NAME(S) AND ADDRESS(ES)

10. SPONSOR/MONITOR'S ACRONYM(S)
AFRL/VSBXS

11. SPONSOR/MONITOR'S REPORT NUMBER(S)

12. DISTRIBUTION / AVAILABILITY STATEMENT
Approved for Public Release; Distribution Unlimited.

*Osservatorio Astro di Palermo, Italy, **Harvard Smithsonian Ctr for Astrophys, Cambridge, MA #NRL, Washington, DC, ##Inst for Astronomy, Univ of Hawaii, Honolulu, HI

13. SUPPLEMENTARY NOTES
REPRINTED FROM: THE ASTROPHYSICAL JOURNAL, Vol 621, pp 1121-1128, March 10, 2005.

14. ABSTRACT

A fast partial-halo coronal mass ejection (CME) was observed on 2000 June 28 by instruments on the *SOHO* spacecraft. The CME leading edge and filamentary cold core were detected over the northwest limb at 2.32 $R_\odot$ by the *SOHO* UV Coronagraph Spectrometer (UVCS). The broad profile of the O VI λ1032 line gives evidence of a shock front at the leading edge, supporting the identification of white-light CME sharp leading edges as fast-mode shocks. Line-of-sight speeds are as high as 1500 km s^{-1}, comparable to the projected speed obtained from LASCO. Pumping of the O VI λ1032 by Lyβ ($v = 1810$ km s^{-1}) and of O VI λ1037 by O VI λ1032 ($v = 1648$ km s^{-1}) were detected, which provide diagnostics of outflow speed and density. The angle of the ejecta with the plane of the sky is obtained, combining the projected speed from LASCO with the line-of sight-speed, and varies between 7° and 46°. In the latter case the projected height of 2.32 $R_\odot$ was at an actual heliocentric distance of 3.6 $R_\odot$. An associated solar energetic particle (SEP) event was observed at the L1 point following this CME. The abundance and charge-state data are consistent with a gradual shock-accelerated SEP event. A type II radio burst was observed at the same time the shock front was detected by UVCS.

15. SUBJECT TERMS
Sun Corona Corona mass ejections UV radiation

16. SECURITY CLASSIFICATION OF:			17. LIMITATION OF ABSTRACT	18. NUMBER OF PAGES	19a. NAME OF RESPONSIBLE PERSON
a. REPORT		c. THIS PAGE			S. W. Kahler
UNCLAS	UNCLAS	UNCLAS	SAR	10	19b. TELEPHONE NUMBER *(include area code)* 781-377-9665